Discovery of potent and selective 5-azaindazole inhibitors of leucine-rich repeat kinase 2 (LRRK2) - Part 1

Osborne, Joanne; Birchall, Kristian; Tsagris, Denise J. ; Lewis, Stephen J. ; Smiljanic-Hurley, Ela ; Taylor, Debra L.

Published in:
Bioorganic & Medicinal Chemistry Letters

DOI:
10.1016/j.bmcl.2018.11.058

Publication date:
2019

Bioorganic & Medicinal Chemistry Letters 29 (2019) 668–673

Contents lists available at ScienceDirect

Bioorganic & Medicinal Chemistry Letters

journal homepage: www.elsevier.com/locate/bmcl

Discovery of potent and selective 5-azaindazole inhibitors of leucine-rich repeat kinase 2 (LRRK2) – Part 1

Joanne Osborne[a], Kristian Birchall[a], Denise J. Tsagris[a], Stephen J. Lewis[a], Ela Smiljanic-Hurley[a], Debra L. Taylor[a], Alison Levy[a], Dario R. Alessi[b], Edward G. McIver[a,*]

[a] LifeArc, Accelerator Building, Open Innovation Campus, Stevenage SG1 2FX, UK
[b] The MRC Protein Phosphorylation Unit, The Sir James Black Centre, College of Life Sciences, University of Dundee, Dow Street, Dundee DD1 5EH, UK

ARTICLE INFO

Keywords:
Parkinson's disease
G2019S
Kinase inhibitor
LLE

ABSTRACT

Parkinson's disease is a relatively common neurological disorder with incidence increasing with age. Present treatments merely alleviate the symptoms and do not alter the course of the disease, thus identification of disease modifying therapies represents a significant unmet medical need. Mutations in the LRRK2 gene are risk-factors for developing PD and it has been hypothesized that the increased kinase activity of certain LRRK2 mutants are responsible for the damage of the dopaminergic neurons, thus LRRK2 inhibitors offer the potential to target an underlying cause of the disease. In this communication, we describe hit-to-lead medicinal chemistry program on a novel series of 5-azaindazoles. Compound **1**, obtained from high-throughput screening was optimized to a highly potent, selective series of molecules with promising DMPK properties. Introduction of heterocycles at the 3-position were found to significantly increase the potency and kinase selectivity, whilst changes to the 4-chlorobenzyl group improved the physicochemical properties. Our series was licensed to a major pharmaceutical company for further development.

Parkinson's Disease (PD) is a neurodegenerative disorder affecting approximately 1–2% of the population at 60 years of age.[1] Symptoms include impaired motor function, tremor, rigidity, impaired balance and speech. The pathological hallmarks for PD include a reduction of dopaminergic neurons and dopamine secretion in the substantia nigra pars compacta region of the brain and the formation of Lewy bodies and intracellular fibrils in neurons. Current therapies are limited to management of the symptoms associated with reduced dopamine signalling, such as L-DOPA therapy which increases the levels of dopamine in the striatum.[2] These treatments have unpleasant side-effects and moreover, they do not address the underlying cause. Therefore, a disease modifying therapy remains a significant unmet medical need for PD.

Although the majority of cases of PD are sporadic, it has been established that mutations in the LRRK2 gene are commonly associated with cases of familial PD.[3] The most prevalent mutation in the protein is G2019S,[4] which is present in the kinase domain and is associated with increased kinase activity in biochemical and cellular assays. It has been hypothesized that the increased kinase activity may be associated with the neurodegeneration and that inhibition of LRRK2 may slow the progression of the disease. There has been considerable interest in this target with a number of groups reporting their LRRK2 inhibitor programs.[5] In this communication we describe the development of a novel series of azaindazole LRRK2 inhibitors.

Our high throughput screening campaign at LifeArc identified a 5-azaindazole derivative **1**. This was an attractive hit, owing to its low MW, good ligand efficiency (LE), lipophilic ligand efficiency (LLE) low PSA and a CNS MPO score of 4.7 with significant potential for further optimization (Fig. 1).[6]

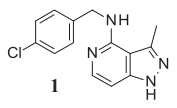

1

LRRK2 IC_{50}	4.9 μM
LLE, LE	2.0, 0.38
MW, cLogP	272, 3.3
TPSA	54 $Å^2$

Fig. 1. HTS screening hit.

We initially focused our attention on varying the 4-chlorobenzyl group (Table 1). An early observation was that the 4-chloroaniline derivative **2** resulted in a significant gain in potency, therefore a range of anilines and amino heterocycles were synthesized (entries **3**–**7**). The most potent example being the 4-methyl aniline derivative **4**, however this compound was found to have modest microsomal stability. Although the heterocyclic analogues (**5**–**7**) had improved

* Corresponding author.

https://doi.org/10.1016/j.bmcl.2018.11.058
Received 16 August 2018; Received in revised form 16 November 2018; Accepted 30 November 2018
Available online 01 December 2018

physicochemical properties, a loss in potency for LRRK2 was observed, with the 3-pyridyl derivative **5** being inactive. A range of non-aromatic amines were also investigated. Directly linked heterocycloalkyl amines, such as the morpholine **8** generally had weak potency, however, the cyclohexyl derivative **9** showed a significant boost in potency compared to the hit. Gratifyingly, this compound also had reasonable microsomal stability, and good CNS penetration in mice with a total brain-plasma ratio of 4:1. The kinase selectivity (Fig. 2) was surprisingly good considering the small size of this compound and was significantly better than the aniline derivative **4**. Further cycloalkylamino derivatives were also investigated and it was found that reducing the ring-size (entries **11–13**) resulted in a progressive loss of potency. Methylation of the cyclohexylamino group (entry **10**) resulted in a significant potency loss. Linear and branched aliphatic amines were also investigated for example, **14–16**, in general these compounds had weak affinity, with the exception of the isobutyl derivative **16**. Of all the amino derivatives that were synthesized, the 4-tetrahydropyranyl derivative **17** had the optimal balance of potency and microsomal stability. Furthermore, this compound was found to have good CNS penetration in mice, with a brain-plasma ratio of 1.6:1.

A range of ether derivatives were also investigated, and in general these were found to be significantly more potent than the corresponding amino derivatives. For example, the cyclohexyl derivative (**18**) showed a 6-fold increase in potency compared to the amino derivative. On the other hand, these compounds were found to have reduced microsomal stability compared to their amino counter-parts, possibly due to their increased lipophilicity. An attempt to reduce the lipophilicity by incorporation of a basic nitrogen in the ring (**20**) resulted in a dramatic loss in potency. However, the more polar tetrahydropyranyl and tetrahydrofuranyl derivatives (**19** and **25**) was found to have significantly improved microsomal stability.

Of the 3-methyl derivatives, compounds **17** and **19** were found to have the best overall balance of potency, selectivity and microsomal stability, which is also reflected in having the highest LLEs of 5.5 and 5.6 respectively.

In order to improve the potency further, we turned our attention to the 3-position (Table 2). This work led to the identification of heterocycles, such as pyrazoles (**26–29**) and the morpholinopyridine **30**, which showed a modest potency boost compared to the corresponding methyl derivatives. The real breakthrough came when switching to the

Table 1
4-Position SAR of some representative examples.

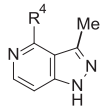

Entry	R^4	LRRK2 IC50 (μM)[a]	cLogP/LLE	HLM/MLM % turn.[b]	Entry	R^4	LRRK2 IC50 (μM)[a]	cLogP /LLE	LogD7.4	HLM/MLM % turn[b]
2	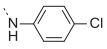	0.39	3.6/3.9	-/-	**14**		0.88	2.0/4.1	–	-/-
3	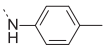	0.097	3.1/3.9	13/28	**15**		2.4	2.0/3.6	–	-/-
4		0.15	3.3/3.5	-/-	**16**		0.30	2.5/4.0	–	6/9
5		> 10	1.7/-	-/-	**17**		0.19	1.1/5.5	1.2	0/4
6	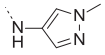	0.83	1/5.1	-/-	**18**		0.067	4.0/3.2	> 4	25/37
7	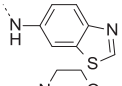	0.38	2.4/4.0	-/-	**19**	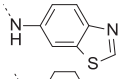	0.13	1.3/5.6	2.2	8/11
8		3	0.5/5.0	-/-	**20**	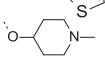	1.9	1.7/4.0	–	-/-
9		0.39	3.2/3.2	7/13	**21**		0.44	1.9/4.4	–	-/-
10		1.6	3.5/2.3	-/-	**22**		0.068	3.2/4.0	–	2/24
11		0.41	2.6/3.8	2/10	**23**		0.086	2.9/4.2	–	31/42
12		0.53	2.1/4.1	-/-	**24**		0.17	3.5/3.2	–	22/41
13		4.7	1.5/3.8	-/-	**25**		0.25	1.2/5.4	–	0/13

[a] Radiometric assay using G2019S LRRK2 protein from Invitrogen. The values quoted are the mean of at least 2 experiments and with a range of < 25% of the mean.

[b] Values relate to % turnover of compound following *in vitro* incubation with human liver microsomes (HLM) for 40 min or mouse liver microsomes (MLM) for 30 min.

Compound	LRRK2 IC50 (μM)	Concentration (μM)	Kinase Selectivity Heat Map	RGM Score
4	0.38	10		0.57
9	0.39	10		0.61
18	0.066	10		0.36
19	0.13	10		0.59
32	0.011	1		0.74
35	0.012	1		0.92
% Kinase inhibition			>90 75-90 60-75 50-60 <50	

Fig. 2. Kinase selectivity heat map for a selection of compounds against a panel of 59 protein kinases at the specified concentration. The Rescaled geometric mean gives a numerical score between 0.1 (highly promiscuous) to 1 (highly selective).

Table 2
Selection of 3-heteroaryl analogues.

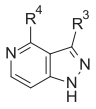

Entry	R^4	R^3	LRRK2 IC_{50} (μM)[a]	PSA (Å^2)	cLogP/LLE	$mLogD_{7.4}$	HLM/MLM % turn.[b]
26			0.13	71	2.8/4.1	2.7	21/19
27			0.11	71	3.7/3.3	3.2	23/43
28		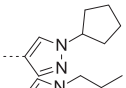	0.17	81	2.2/4.6	–	-/-
29		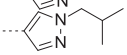	0.41	81	2.1/4.3	–	-/-
30		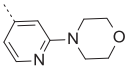	~	88	0.9/6.2	–	17/11
31		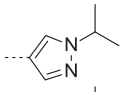	0.002	69	3.9/4.8	3.7	36/66
32		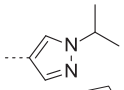	0.011	78	1.8/6.2	–	21/20
33		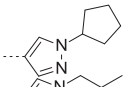	0.004	78	2.4/6.0	–	-/-
34		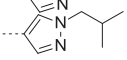	0.015	78	2.3/5.5	–	-/-
35		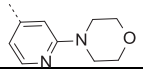	0.012	85	1.1/6.7	–	43/19

[a] Radiometric assay using G2019S LRRK2 protein from Invitrogen. The values quoted are the mean of at least 2 experiments and with a range of < 25% of the mean.

[b] Values relate to % turnover of compound following *in vitro* incubation with human liver microsomes (HLM) for 40 min or mouse liver microsomes (MLM) for 30 min. Values given are the mean of at least two experiments.

ether analogues (**31–35**). The cyclohexyloxy derivative **31** displayed a 55-fold boost in potency compared to the corresponding cyclohexylamino derivative **27**. Unfortunately this compound and related analogues suffered from poor microsomal stability, possibly due to the relatively high LogD. Switching to the 4-tetrahydropyranyl ether, yielded compounds with improved physicochemical properties, such as the isopropyl pyrazole **32** pyridylmorpholine **35**.

Fig. 2 shows the selectivity data for a selection of compounds

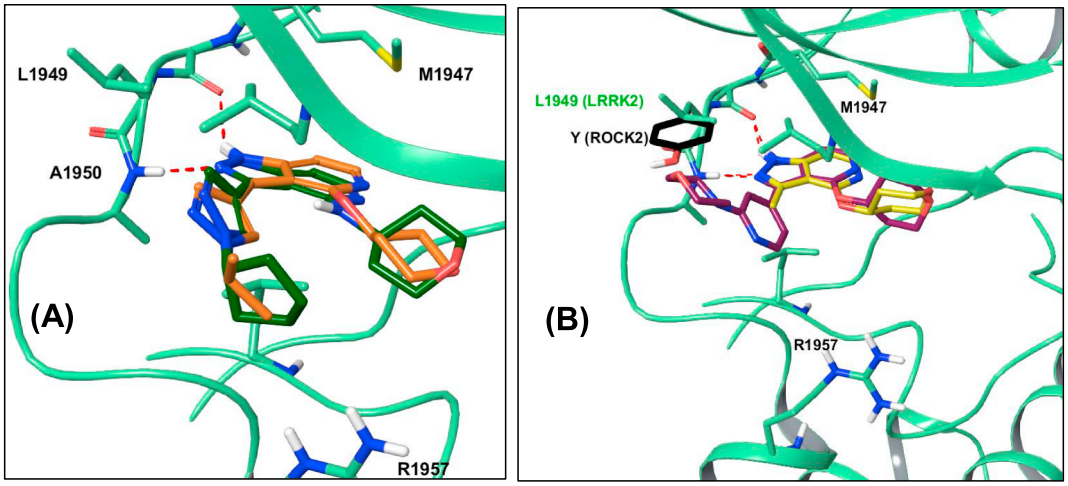

Fig. 3. A) Predicted binding mode of 28 (dark green) and 32 (orange) to ATP-binding site of LRRK2 homology model; B) Predicted binding modes of 17 (yellow) and 35 (purple) to ATP-binding site of LRRK2 homology model; the LRRK2 residues are shown in light green and mutated L1949Y residue is shown in black which exists in, for example ROCK2. Extending out from the 3-position of the azaindazole is well tolerated in LRRK2 but clashes with Y and F hinge-residues and hence these compounds are more selective. These homology models were generated using the Prime module of Schrodinger Suite 7 and were based on the crystal structure of JAK2 (PDB: 1YVJ). Dockings were carried out using GlideSP1 with H-bonding constraints to E1948 and A1950.

Table 3
Selection of core modifications to probe the hinge-interaction.

Entry	Compound	LRRK2 IC_{50} (μM)[a]
36	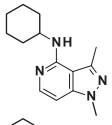	> 10
37	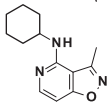	> 10
38	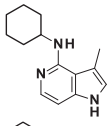	> 10
39	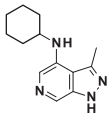	0.77

[a] Radiometric assay using G2019S LRRK2 protein from Invitrogen. The values quoted are the mean of at least 2 experiments and with a range of < 25% of the mean.

against a panel of 59 protein kinases. The rescaled geometric mean (RGM) gives an indication of how selective the compound is, and a score of > 0.7 is considered to be highly selective.[7] The 4-anilino derivatives, such as **4** were found to have inferior selectivity to the corresponding cyclohexylamino derivative **9**. Interestingly the 4-THP derivatives appear to be more selective than the corresponding 4-cyclohexyloxy analogues (**18** versus **19**), which is reflected in a marked improvement of the RGM. Gratifyingly the selectivity of the 3-heteroaryl analogues, including **32** and **35** improved dramatically. The improvement in selectivity is due to LRRK2 possessing a leucine residue (L1949) at the hinge region which can easily accommodate compounds with a wide range of larger substituents on the 3-position. Sequence alignment carried out by Genentech confirms that the majority of kinases possess larger residues, such as phenylalanine or a tyrosine at the same position,[8] which can easily accommodate compounds bearing the 3-methyl substituent, such as **18** and **19**. Extending out from the 3-position results in an unfavourable steric clash with these Phe and Tyr residues (Fig. 2B). We carried our own sequence alignments of LRRK2 with significant kinases inhibited by compounds **18** and **19**, including RSK1, ROCK2, PIM1, GSK3β, CDK2 and MSK1 using the sequence alignment tool in BioLuminate 1.9. Comparison of the selectivity data of **19** and **32** backs up this hypothesis: kinases most significantly inhibited by compound **32** are PIM1 (77%) and GSK3β (90%), both of which also possess Leu residues at this position. On the other hand, kinases bearing larger residues such as ROCK2(Tyr), CDK2(Phe) and MSK1(Tyr) were significantly inhibited by **18** and **19** but had much lower inhibition by **32** and **35.**

Fig. 3A shows docking of key compounds into the hinge region of a LRRK2 homology model. We believe that the indazole forms two H-bonding interactions with E1948 and A1950 at the hinge, with the pyrido ring occupying the hydrophobic pocket in close proximity to the M1947 gatekeeper residue. The heterocycle coming off the 3-position of the core forms favourable interactions with the shallow hydrophobic pocket approaching the solvent channel. Ether derivatives, such as **32** appear to position the tetrahydropyranyl ring more tightly within the pocket under the glycine-rich loop and becoming less solvent exposed than the amine derivatives, such as **28**. In this case the THP-ring appears to rotate further out of plane with the core and forms a less favourable interaction with protein. The improved selectivity of compounds with larger substituents in the 3-position can be rationalised by mutation of the L1949 residue to a Y (Fig. 3B). Relatively few kinases, including LRRK2 have small or medium sized residues at this position which can easily accommodate bulky heterocyclic substituents. On the other hand, the majority of kinases bear larger phenylalanine or tyrosine residues in the same position which form unfavourable steric interactions with these ligands. To further confirm the proposed hinge-binding mode we investigated a range of single point changes on the core (Table 3). Removal of the H-donor at N1 was not tolerated, as both the N-methyl azaindazole (**36**) and the 5-azabenzisoxazole (**37**) show a complete loss of activity for LRRK2. Removal of the nitrogen at the 2-position (**38**) was also inactive. The observation that the 6-azaindazole (**39**) retained some activity suggests that it is unlikely that 5-aza nitrogen is involved in hinge-binding. Furthermore, our proposed binding mode is consistent with X-ray crystal structures reported for 5- and 6-substituted indazoles complexed to other kinases (see PDB: 5L3A (JAK2), 3ZLY (MEK), 2UZU (AKT).

Scheme 1 illustrates the synthesis of compounds **1–37**.[9] Grignard addition of MeMgBr to 2,4-dichloropyridine-3-carbaldehyde **40** followed by a Ley-Griffith oxidation gave ketone **41**, which was reacted

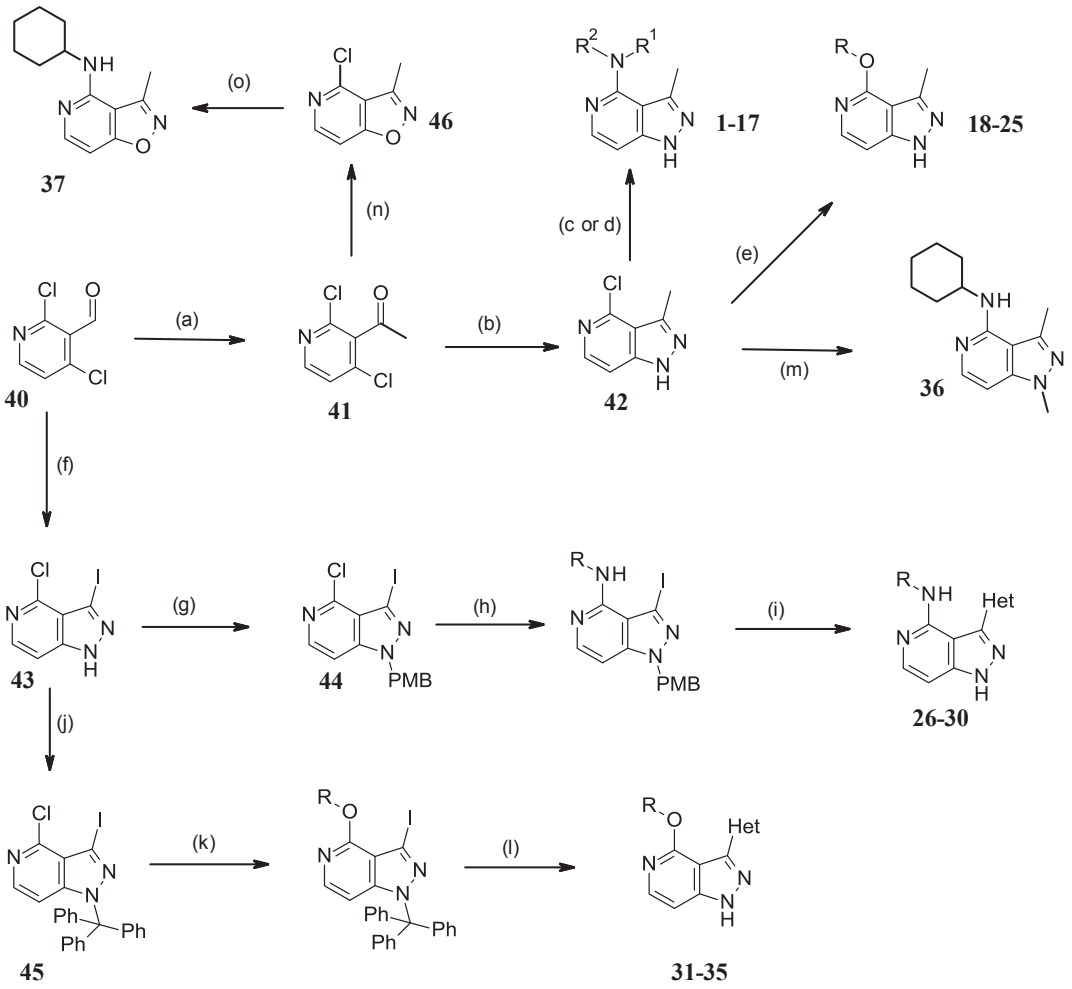

Scheme 1. (a) i. MeMgBr, THF, −78 °C to −20 °C, 73%; ii. TPAP, NMO, DCM, molecular sieves, rt, 80%; (b) $N_2H_4{\cdot}H_2O$, rt, 64%; (c) HNR^1R^2, *n*-butanol or DME, microwave, 190 °C; (d) HNR^1R^2, HCl, *n*-butanol, microwave, 190 °C; (e) R^3OH, NaH, dioxane, rt, then **42**, microwave, 180 °C; (f) i. $N_2H_4{\cdot}H_2O$, rt, 64%; ii. I_2, KOH, dioxane, 70 °C, 61%; (g) *p*-methoxybenzylchloride, KOH, DMF, rt, 93%; (h) HNR^1R^2, HCl, *n*-butanol, microwave, 190 °C; (i) i. Boronic acid or ester, $Pd(dppf)Cl_2$, 2 M Na_2CO_3, dioxane, 90 °C; ii. TFA, 70 °C; (j) Triphenylmethylchloride, NaH, DMF, 0 °C – rt, 96%; (k) ROH, NaH, Dioxane, 0 °C, then **45** microwave, 185 °C; (l) i. Boronic acid or ester, $Pd(dppf)Cl_2$, 2 M Na_2CO_3 dioxane, 90 °C; ii. TFA, DCM, rt; (m) i. NaH, MeI, DMF, rt, 65%; ii. Cyclohexylamine, *n*-BuOH, microwave, 190 °C, 2 h, 38%; (n) i. $NH_2OH.HCl$, pyridine, reflux, 32%; ii. $Pd(OAc)_2$, dppf, NaO^tBu, 50 °C, 21%; (o) Cyclohexylamine (neat), 80 °C, 6 h, 64%.

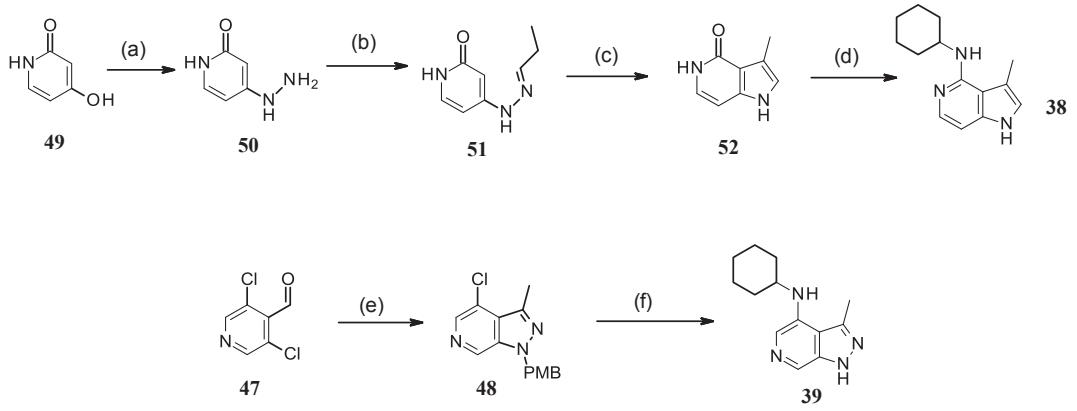

Scheme 2. (a) $N_2H_4{\cdot}H_2O$, 2-methoxyethanol, 125 °C, 71%; (b) propionaldehyde, EtOH, reflux, 45%; (c) Ph_2O, reflux, 7 h, 22%; (d) i. $POCl_3$, 65 °C, 16 h, 81%; ii. $^iPr_2NEt$, NMP, 150 °C, 3%; (e) i. MeMgBr, THF, −78 °C, 61%; ii. TPAP, NMO, DCM, molecular sieves, rt; iii. $N_2H_4{\cdot}H_2O$, *n*-BuOH, 200 °C, microwave, 30 min., 51%; iv. PMBCl, KOH, DMF, rt, 70%; (f) i. $Pd_2(dba)_3$, xantphos, NaO^tBu, cyclohexylamine, dioxane; ii. $AlCl_3$, toluene, 50 °C, 4 h, 12% (2 steps).

with hydrazine to give the chloroheterocycle **42.** Nucleophilic substitution of **42** with the appropriate amine gave the desired 4-amino derivatives **1–17**. Ether derivatives **18–25** can be prepared by nucleophilic displacement with the corresponding sodium alkoxide with microwave heating. Condensation of **41** with hydroxylamine to the oxime followed palladium mediated cyclisation gave **46,** which was reacted with cyclohexylamine to furnish the 6-azabenzisoxazole derivative **37**. Alternatively, **40** can be converted to 3-iodo-4-chloro-5-

azaindazole **43,** a versatile intermediate enabling variation of both the 3- and 4-positions. To facilitate palladium mediated couplings to the 3-iodo group, it was necessary to introduce a suitable protecting group to the indazole NH as in the absence of protection, the subsequent couplings were found to be low yielding. The 4-amino derivatives **26–30** were synthesized *via* nucleophilic displacement of PMB-protected intermediate **44**, followed by Suzuki-coupling of the appropriate boronic acid or boronic ester. Deprotection using TFA gave the desired compounds. We found that the PMB-protecting group was incompatible with the ether derivatives, as the conditions required for removal were too harsh. Much higher yields could be obtained from the trityl intermediate **45**, as deprotection takes place under much milder conditions. Thus **45** can be converted to the corresponding 4-alkoxy-5-iodo intermediates, which in turn will undergo Suzuki couplings. Finally, deprotection with TFA at room-temperature in DCM yielded the desired ether derivatives **31–35**. The N-methyl-5-azaindazole **36** was prepared in 2 steps by methylation of **42** followed by displacement with cyclohexylamine.

Scheme 2 illustrates the syntheses of the 5-aza-indole **38** and the 6-azaindazole **39**. The 5-azaindole derivative was prepared using a modified Fischer-indole synthesis. Chlorodehydration of **52** followed by displacement with cyclohexylamine gave **38**. Commercially available aldehyde **47** was converted to the PMB-protected 4-chloro-6-azaindazole intermediate **48** in three steps using similar chemistry described above. Buchwald coupling of **48** with cyclohexylamine gave the corresponding PMB-protected amine, which was deprotected with aluminium chloride to give **38**. All final compounds were purified by mass-directed HPLC.

In conclusion we have optimized a weakly active HTS hit **1** into a promising lead series of potent and selective LRRK2 inhibitors with promising DMPK properties. Introduction of heterocycles at the 3-position was found to significantly increase the potency and kinase selectivity, whilst changes to the 4-chlorobenzyl group improved the physicochemical properties. The compounds also show excellent CNS penetration. LifeArc is a UK based technology transfer organization performing translational research in collaboration with leading academic groups. These compounds were sufficiently promising for a large pharmaceutical company to license the series from us and their optimization efforts will be discussed in a separate communication.

Acknowledgments

The authors would like to acknowledge Hilary McLauchlin and James Hastie of MRC Protein Phosphorylation unit for coordinating and running the kinase selectivity assays. In vitro DMPK assays were run by David Tickle and Sadhia Khan of LifeArc. The PK study was carried out by Pharmadex, and certain compounds and intermediates were synthesized by GVK. We would also like to thank Zach Sweeney and Anthony Estrada for useful discussion.

Appendix A. Supplementary data

Supplementary data to this article can be found online at https://doi.org/10.1016/j.bmcl.2018.11.058.

References

1. (a) Lees AJ, Hardy J, Revesz T. Parkinson's disease. *Lancet.* 2009;373(9680):2055–2066
   (b) Lim KL, Zhang CW. Molecular events underlying Parkinson's disease – an interwoven tapestry. *Front Neurol.* 2013;4:33
   (c) Martinez-Martin P, Kurtis MM. Health-related quality of life as an outcome variable in Parkinson's disease. *Ther Adv Neurol Disord.* 2012;5(2):105–117.
2. Connolly BS, Lang AE. Pharmacological treatment of Parkinson disease: a review. *JAMA.* 2014;311(16):1670–1683.
3. (a) Marin I. The Parkinson disease gene LRRK2: evolutionary and structural insights. *Mol Biol Evol.* 2006;23(12):2423–2433
   (b) Mata IF, Wedemeyer WJ, Farrer MJ, Taylor JP, Gallo KA. LRRK2 in Parkinson's disease: protein domains and functional insights. *Trends Neurosci.* 2006;29(5):286–293
   (c) Paisan-Ruiz C, Jain S, Evans EW, et al. Cloning of the gene containing mutations that cause PARK8-linked Parkinson's disease. *Neuron.* 2004;44(4):595–600
   (d) Zimprich A, Biskup S, Leitner P, et al. Mutations in LRRK2 cause autosomal-dominant parkinsonism with pleomorphic pathology. *Neuron.* 2004;44(4):601–607.
4. Clark LN, Wang Y, Karlins E, et al. Frequency of LRRK2 mutations in early- and late-onset Parkinson disease. *Neurology.* 2006;67(10):1786–1791.
5. (a) Chan BK, Estrada AA, Chen H, et al. Discovery of a Highly Selective, Brain-Penetrant Aminopyrazole LRRK2 Inhibitor. *ACS Med Chem Lett.* 2013;4(1):85–90
   (b) Estrada AA, Chan BK, Baker-Glenn C, et al. Discovery of highly potent, selective, and brain-penetrant aminopyrazole leucine-rich repeat kinase 2 (LRRK2) small molecule inhibitors. *J Med Chem.* 2014;57(3):921–936
   (c) Estrada AA, Liu X, Baker-Glenn C, et al. Discovery of highly potent, selective, and brain-penetrable leucine-rich repeat kinase 2 (LRRK2) small molecule inhibitors. *J Med Chem.* 2012;55(22):9416–9433
   (d) Hatcher JM, Zhang J, Choi HG, Ito G, Alessi DR, Gray NS. Discovery of a Pyrrolopyrimidine (JH-II-127), a Highly Potent, Selective, and Brain Penetrant LRRK2 Inhibitor. *ACS Med Chem Lett.* 2015;6(5):584–589
   (e) Henderson JL, Kormos BL, Hayward MM, et al. Discovery and preclinical profiling of 3-[4-(morpholin-4-yl)-7H-pyrrolo[2,3-d]pyrimidin-5-yl]benzonitrile (PF-06447475), a highly potent, selective, brain penetrant, and in vivo active LRRK2 kinase inhibitor. *J Med Chem.* 2015;58(1):419–432
   (f) Troxler T, Greenidge P, Zimmermann K, et al. Discovery of novel indolinone-based, potent, selective and brain penetrant inhibitors of LRRK2. *Bioorg Med Chem Lett.* 2013;23(14):4085–4090.
6. (a) Kuntz ID, Chen K, Sharp KA, Kollman PA. The maximal affinity of ligands. *PNAS.* 1999;96(18):9997–10002
   (b) Leeson PD, Springthorpe B. The influence of drug-like concepts on decision-making in medicinal chemistry. *Nat Rev Drug Discovery.* 2007;6(11):881–890
   (c) Shultz MD. Setting expectations in molecular optimizations: Strengths and limitations of commonly used composite parameters. *Bioorg Med Chem Lett.* 2013;23(21):5980–5991
   (d) Shultz MD. Improving the plausibility of success with inefficient metrics. *ACS Med Chem Lett.* 2014;5(1):2–5
   (e) Wager TT, Hou X, Verhoest PR, Villalobos A. Moving beyond rules: the development of a central nervous system multiparameter optimization (CNS MPO) approach to enable alignment of druglike properties. *ACS Chem Neurosci.* 2010;1(6):435–449.
7. Wang X, Greene N. Comparing Measures of Promiscuity and Exploring Their Relationship to Toxicity. *Mol Inf.* 2012;31(2):145–159.
8. Chen H, Chan BK, Drummond J, et al. Discovery of selective LRRK2 inhibitors guided by computational analysis and molecular modeling. *J Med Chem.* 2012;55(11):5536–5545.
9. McIver EG, Smiljanic E, Harding DJ, Hough J, Preparation of pyrazolopyridine compounds as kinase inhibitors, WO 2010106333.